Enhanced dissociation of H_2^+ into highly excited states by UV pulses

Kunlong Liu, Qianguang Li, Pengfei Lan & Peixiang Lu

Taylor & Francis
Taylor & Francis Group

RESEARCH ARTICLE

Enhanced dissociation of H_2^+ into highly excited states by UV pulses

Kunlong Liu[a], Qianguang Li[b], Pengfei Lan[a,c] and Peixiang Lu[a,c,*]

[a]*School of Physics and Wuhan National Laboratory for Optoelectronics, Huazhong University of Science and Technology, Wuhan, China;* [b]*School of Physics and Electronic-information Engineering, Hubei Engineering University, Xiaogan, China;* [c]*School of Science, Wuhan Institute of Technology, Wuhan, China*

We theoretically study the dissociation of H_2^+ by UV laser pulses as a function of the photon energy ω of the pulse. Our results show that pronounced enhancements of the dissociation into highly excited electronic states can be achieved at some critical ω. This is found to be attributed to a consecutively resonant excitation mechanism where the population is first transferred to the first excited state by absorbing one photon and then to higher states by absorbing another one or more photons at the same internuclear distance. This study indicates that the strong coupling between the lowest two states of H_2^+ can significantly affect the dissociation through higher lying states.

Keywords: molecular dissociation; resonant excitation; highly excited states; UV laser pulses

1. Introduction

Understanding the electronic excitation and nuclear motion in laser–molecular interaction is of vital importance in controlling the formation and fracture of chemical bonds with laser fields [1–5]. For more than two decades, many efforts have been made to study the dissociation of small molecules exposed to various laser pulses [6–12]. Most of the studies are focused on the interplay of the population between the lowest two electronic states of H_2^+, i.e. the ground ($1s\sigma_g$) and first excited ($2p\sigma_u$) states. For many famous mechanisms, such as bond softening [13], above-threshold dissociation (ATD) [14], asymmetric electron localisation [15], charge-resonance-enhanced ionisation [16–18], and so on, the $H^+ +H(1s)$ dissociation channel of H_2^+ plays the major role in determining the features of the observed fragmentation phenomena. Nevertheless, the role of highly excited states has attracted people's attention since recent works [19–27] revealed more details of the molecular fragmentation processes (e.g. multiphoton dissociative excitation [19,20], high-order ATD [21], and Coulomb explosion without double ionisation [22]) and suggested that the dissociation through highly excited electronic states is a ubiquitous phenomenon in laser–molecular interactions.

In an infrared field, however, it is shown that the contribution from highly excited states to the total dissociation is two orders smaller than that from the $1s\sigma_g$ and $2p\sigma_u$ states [26]. This is, on one hand, due to the weak multiphoton coupling between the $1s\sigma_g$ and highly excited states [19] as well as the ac Stark shifts of the energy levels [28]. On the other

hand, the high ionisation rate of highly excited states would also lead to the decrease of the population of those states [19,29]. As a result, the effects of the population dynamics in high-lying dissociative states are largely weakened and drowned by the $H^+ +H(1s)$ channel, making the study or control of the high-lying dissociative population dynamics difficult.

As the lowest two states of H_2^+ are strongly coupling and well isolated from other states, it is widely considered that the role of highly excited states in H_2^+ dissociation can be ignored. Here, however, we will show that the strong coupling of the lowest two states will significantly affect the dissociation through higher lying states. In this paper, we study the dissociation of H_2^+ by UV pulses and report a novel fragmentation process which leads to pronounced enhancement of the dissociative population in highly excited states. In contrast to the previous study [30], where the population is transferred to higher electronic states via single-photon excitation, the high-lying population in this study is created through a consecutively resonant excitation (CRE) process: for a critical photon energy, the population would be first transferred to the $2p\sigma_u$ state and then to higher states at the same internuclear distance. Our results show that by taking advantage of the strong coupling between the $1s\sigma_g$ and $2p\sigma_u$ states, the multiphoton transition through the CRE process exhibits much higher excitation rate than the direct multiphoton transition. The underlying mechanism has been verified by the nuclear kinetic energy release (KER) spectra for individual dissociative electronic states.

---

*Corresponding author. Email: lupeixiang@mail.hust.edu.cn

2. Theoretical model

For numerical simulations, we have solved the non-Born–Oppenheimer time-dependent Schrödinger equation (TDSE) for a reduced dimensionality model of H_2^+ [31,32]. The model consists of one-dimensional motion of the nuclei and one-dimensional motion of the electron, and the electronic and nuclear motions are restricted along the polarisation direction of the linearly polarised laser pulse. To date, this model has been widely used to study and identify the molecular fragmentation in strong fields [26,27,33–37]. Within this model, the length gauge TDSE can be written as (atomic units are used throughout unless otherwise indicated) $i\frac{\partial}{\partial t}\Psi(R, z; t) = [H_0 + \varepsilon(t)z]\Psi(R, z; t)$, where $H_0 = -\frac{1}{m_p}\frac{\partial^2}{\partial R^2} - \frac{1}{2}\frac{\partial^2}{\partial z^2} + \frac{1}{R} + V_e(z, R)$ with $V_e(z, R)$ being the improved soft-core potential that reproduces the exact $1s\sigma_g$ potential curve in full dimensions [32]. Here, R is the internuclear distance, z is the electron position measured from the centre-of-mass of the protons, and m_p is the mass of the proton. The laser electric field is given by $\varepsilon(t) = \varepsilon_0 \sin^2(\pi t/T_d)\sin(\omega t)$ $(0 < t < T_d)$ with T_d, ω, and ε_0 being the full pulse duration, the central frequency, and the peak electric field amplitude, respectively.

The TDSE is solved on a grid by using the Crank–Nicolson split-operator method with a time step of $\Delta t = 0.04$ au. The grid ranges from 0 to 40 au for R and from -200 to 200 au for z, with grid spacings of $\Delta R = 0.05$ au and $\Delta z = 0.2$ au. After the pulse is off, the wave function of the jth electronic state can be obtained by projecting the final wave function to the electronic bound state $\Psi_e^j(z; R)$ at each fixed internuclear distance, i.e.

$$\Psi_D^j(z; R) = \langle\Psi(z; R)|\Psi_e^j(z; R)\rangle\Psi_e^j(z; R), \quad (1)$$

where j equals to 0, 1, 2, ... and indicates the ground state, the first excited state, the second excited state, and so on.

Then, the integration of $\Psi_D^j(R, z)$ produces the probability of the population in the jth electronic state.

To verify the dynamical mechanism of the dissociation, the nuclear KER spectrum for the dissociation channel through a specific electronic state is needed. In this work, we calculate the channel-specific KER spectra by utilising the energy window operator [38]. In detail, a channel-specific energy window operator is defined by

$$\hat{W}^j(E_N) = \delta^{2k}/[(\hat{H}_N^j - E_N)^{2k} + \delta^{2k}], \quad (2)$$

where δ and k are the characteristic parameters of the operator and $\hat{H}_N^j = -\frac{1}{m_p}\frac{\partial^2}{\partial R^2} + [V_N^j(R) - V_N^j(R = \infty)]$ with $V_N^j(R)$ being the R-dependent potential energy of the jth electronic state of H_2^+. Then, the probability distribution for the nuclei having a kinetic energy E_N and the electron being in the jth state is extracted from $\Psi_D^j(R, z)$ by applying the energy window operator at each z, i.e.

$$p^j(E_N; z) = \langle\Psi_D^j(R; z)|\hat{W}^j(E_N)|\Psi_D^j(R; z)\rangle. \quad (3)$$

Finally, the probability density at E_N of the KER spectrum is given by

$$\rho^j(E_N) = \frac{1}{c}\int p^j(E_N, z)dz, \quad (4)$$

with $c = \delta\frac{\pi}{k}\csc(\frac{\pi}{2k})$. In the simulation, the parameters of $\delta = 0.004$ and $k = 2$ are used [39].

3. Results and discussion

Figure 1 shows the probabilities of the dissociation into highly excited electronic states (solid curves) and the total probability of the lowest two states (dashed curves) as a
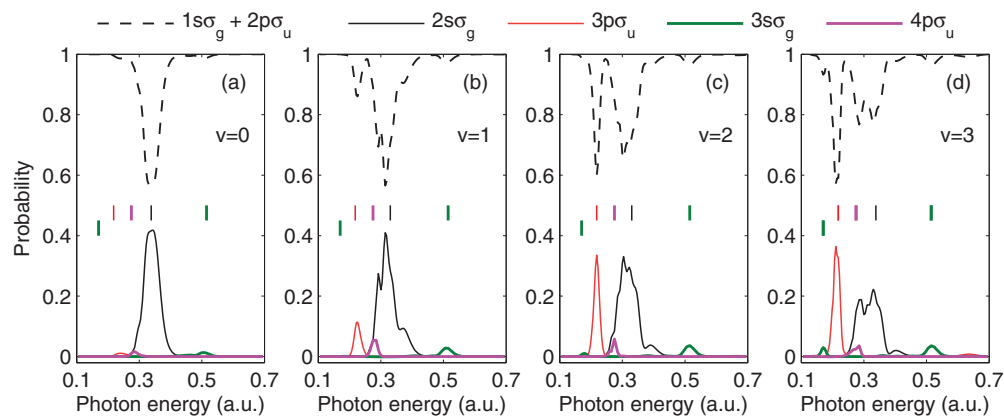
Figure 1. The probabilities of the dissociation into highly excited electronic states (solid curves) and the total probability of the lowest two states (dashed curves) as a function of photon energy of the pulse for the interaction of H_2^+ ($v = 0$–3) with the UV pulses. The pulse intensity is 3×10^{13} W/cm^2 and the pulse duration is 25 optical cycles. The fixed vertical short lines indicate the approximate locations of the dissociation enhancements.

function of pulse frequency ω for the interaction of H_2^+ with the UV pulse. The first four vibrational states ($v = 0$–3) of H_2^+ ($1s\sigma_g$) are chosen as the initial states of Figure 1(a)–1(d), respectively. In the present simulation, the pulse intensity of 3×10^{13} W/cm^2 and $T_d = 25(2\pi/\omega)$ are used and ω ranges from 0.114 to 0.7 au (corresponding to the pulse wavelengths from 400 to 65 nm). Under the pulse parameters that we use here, the ionisation is found to be negligible; thus, we will focus on the population of the electronic bound states.

As shown in Figure 1, the total probability of the $1s\sigma_g$ and $2p\sigma_u$ states (dashed curves) is not conserved as the photon energy varies, indicating that the interplay including only the lowest two states would no longer account for the underlying dynamics even in the case of negligible ionisation. More surprisingly, the remarkable enhancements of the dissociation into the highly excited states ($2s\sigma_g$, $3p\sigma_u$, $3s\sigma_g$, and $4p\sigma_u$) are observed at some critical photon energies. Moreover, the position of the enhancement for each high-lying state is found to be almost independent on the initial states, whereas the maxima of the dissociation probabilities of different excited states exhibit different tendencies as the vibrational state rises. For instance, the maximum probability of $2s\sigma_g$ (thin black curve) tends to decrease with the vibrational states, but the tendency for $3p\sigma_u$ (thin red curve) is opposite.

In order to understand the features of the anomalous dissociation probability shown in Figure 1, here we define the transition location $R_t(\omega)$, which represents the internuclear distance where the resonant excitation channel from $1s\sigma_g$ to the excited state opens, as a function of the photon energy ω. Then, based on the R-dependent potential energies of the electronic states of H_2^+, we calculated the transition location $R_t(\omega)$ for the following transition channels [due to parity considerations, coupling between $1s\sigma_g$ and excited gerade (ungerade) electronic states only occurs in even (odd) numbers of photons]:
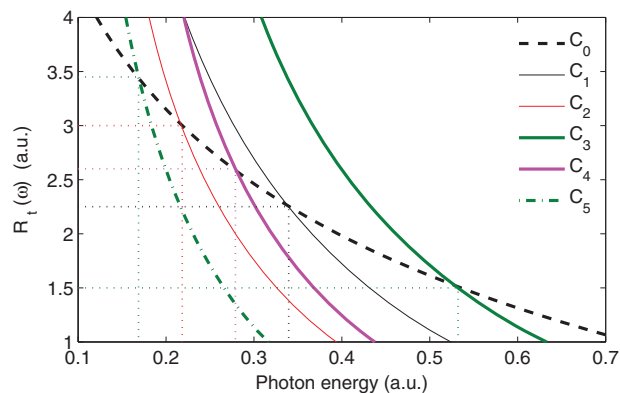
$$C_0: \ 1s\sigma_g + \omega \rightarrow 2p\sigma_u,$$
$$C_1: \ 1s\sigma_g + 2\omega \rightarrow 2s\sigma_g,$$
$$C_2: \ 1s\sigma_g + 3\omega \rightarrow 3p\sigma_u,$$
$$C_3: \ 1s\sigma_g + 2\omega \rightarrow 3s\sigma_g,$$
$$C_4: \ 1s\sigma_g + 3\omega \rightarrow 4p\sigma_u,$$
$$C_5: \ 1s\sigma_g + 4\omega \rightarrow 3s\sigma_g.$$

The results have been shown in Figure 2. One can see that the curve of C_0 (dashed) and other curves intersect at different coordinates, respectively, as indicated by the dotted lines. Note that the crossing of two curves of $R_t(\omega)$ in Figure 2 means that under the photon energy of the crossing, the two represented transition channels would open at the same internuclear distance. By comparing the results of Figures 1 and 2, we find that the abscissa values of the crossings in Figure 2 are approximately equal to those critical photon energies that lead to the enhanced dissociation
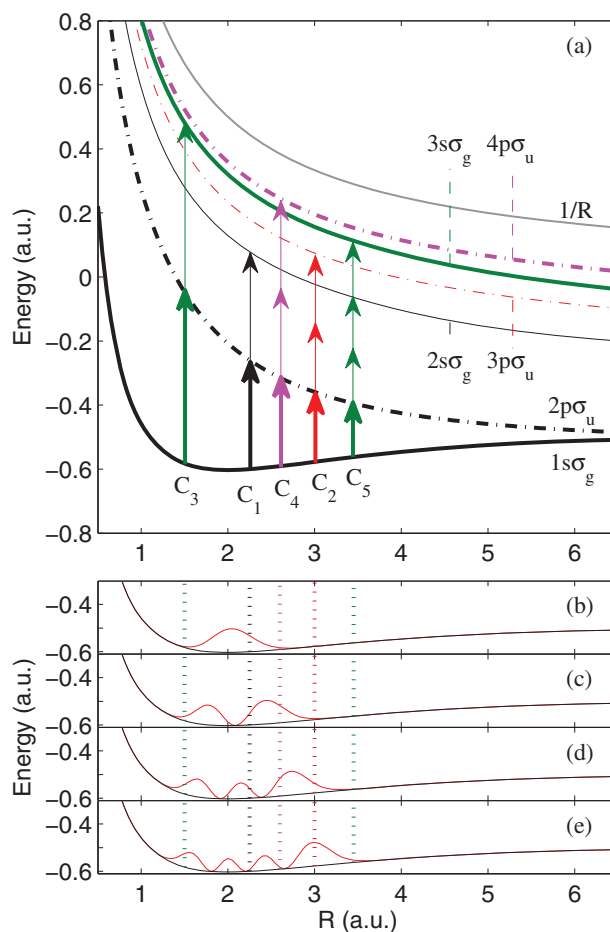

Figure 3. (a) Illustration of the CRE mechanism. (b)–(e) The nuclear wave packet profiles on the $1s\sigma_g$ curve for the first four vibrational states of H_2^+. The thick arrows in (a) indicate the overlap of the C_0 channel and other resonant transition channels.

Figure 2. The transition location $R_t(\omega)$ as a function of photon energy ω for the resonant transition channels C_0–C_5 given in the text. The dotted lines illustrate the coordinates of the crossings.

shown in Figure 1. Thus, we suggest that, if the resonant excitation channels to the $2p\sigma_u$ state and to the other highly excited state occur at the same internuclear distance and under the same photon energy, the dissociative population of the corresponding state would be significantly increased.

Based on the above analysis, we now reveal the underlying physical mechanism with the diagram of the molecular potential curves. Figure 3(a) illustrates the resonant transition channels C_1–C_5 that lead to the enhanced dissociation into the highly excited states. The critical photon energies and transition locations for these channels are given by the respective crossings shown in Figure 2. It can be seen in Figure 3(a) that the first photon absorption of each channel overlaps with the corresponding C_0 channel. In this situation, the direct multiphoton transition becomes a two-step transition process; that is, the molecule is firstly excited to $2p\sigma_u$ by absorbing one photon and sequentially to higher states by absorbing another one or more photons at the same internuclear distance. We call this process the CRE. For the first step of the excitation, due to the strong coupling between the lowest two states, remarkable population would be transferred from $1s\sigma_g$ to $2p\sigma_u$. Then, for the second step, because the coupling of $2p\sigma_u$ to the higher states is stronger than that of the $1s\sigma_g$ state, the excited population in $2p\sigma_u$ would be efficiently transferred to the higher state

before it dissociates to larger internuclear distance. As a result, the multiphoton transition through the CRE process would exhibit much higher excitation rate than the direct multiphoton transition.

Furthermore, besides the excitation rate, the distribution of the initial nuclear wave packet would affect the yield of the excited population [27]. In Figure 3(b)–3(e), we illustrate the nuclear wave packet profiles on the $1s\sigma_g$ curve for the first four vibrational states of H_2^+. For $v = 0$, the wave packet concentrates around $R = 2$ au, so only the dissociative population through the C_1 channel is significantly enhanced (see Figure 1(a)). For higher vibrational states, the probability distribution expands to a wider distribution in R dimension. Thus, the enhancements of other CRE channels gradually become pronounced. In contrast, as the vibrational state rises, the wave packet distribution around the C_1 channel is decreased and becomes modulated; thus, the maximum dissociation probability of $2s\sigma_g$ decreases and the modulation structure appears in the probability curve (thin black) of $2s\sigma_g$ (see Figure 1(d)).

Next, in order to substantiate the CRE mechanism proposed above, we calculated the channel-specific KER spectra of the dissociation into the first five excited electronic states ($2p\sigma_u$, $2s\sigma_g$, $3p\sigma_u$, $3s\sigma_g$, and $4p\sigma_u$). The results for the interaction of H_2^+ ($v = 2$) with the UV pulses
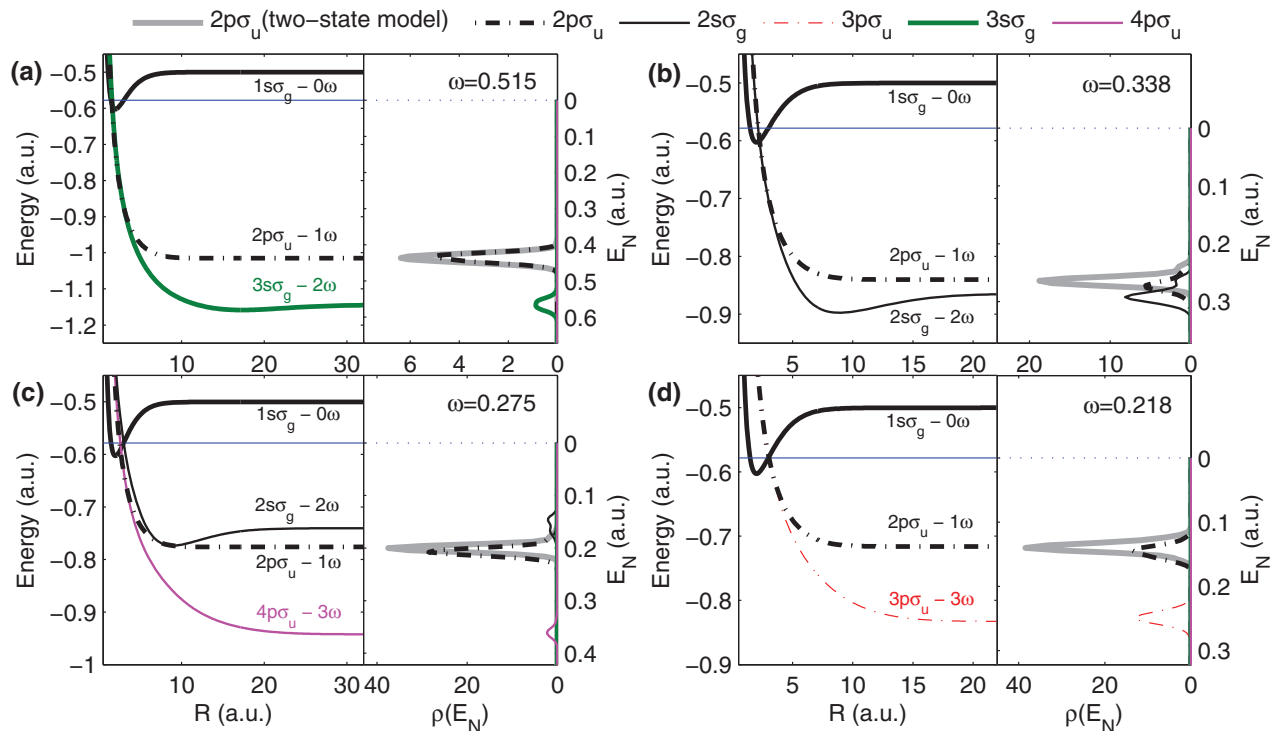

Figure 4. The dressed molecular potential curves (left-hand panels) and the channel-specific KER spectra of the dissociation into the first five excited electronic states (right-hand panels) by UV pulses. The pulse frequencies are given in the corresponding panels and the other pulse parameters are the same as in Figure 1. The solid horizontal lines in the left-hand panels indicate the initial vibrational energy of H_2^+ ($v = 2$).

of four critical photon energies have been shown in the right-hand panels of Figure 4(a)–4(d), including the KER spectra of the $2p\sigma_u$ state (thick grey curves) obtained from the two-state model. The chosen photon energies, i.e. $\omega =$ 0.515, 0.338, 0.275, and 0.218 au, would trigger the CRE in the C_3, C_1, C_4, and C_2 channels, respectively, as shown in Figure 3(a). For comparison, the molecular potential curves dressed by the corresponding photon energies are depicted in the left-hand panels of Figure 4(a)–4(d). Note that only the responsible dressed potentials are plotted.

As shown in Figure 4, if only the lowest two states are considered, the peak positions of the KER spectra of $2p\sigma_u$ (thick grey curves) are in good agreement with the predictions of the $2p\sigma_u - 1\omega$ curves. However, as long as the higher excited states are taken into account, the KER spectra of $2p\sigma_u$ (thick dash–dotted curves) deviate from those of the two-state model. Compared to the two-state model, the dissociation yields of $2p\sigma_u$ are lower and the peak positions are shifted in the TDSE calculation. Such deviations indicate that the dissociative population, which was supposed to dissociate along the $2p\sigma_u$ curve after the single-photon transition, have been partially transferred to higher states before it begins to dissociate. As a result, in addition to the spectra of $2p\sigma_u$, the KER spectra peaks of other excited states can also be observed in Figure 4. Moreover, the KER spectra of the highly excited states are found to be in good agreement with the predictions of the responsible dressed potential curves. These results demonstrate that the enhanced dissociation into highly excited states arises from the CRE process.

Additionally, we notice that there is an enhancement in the KER spectrum for the $2s\sigma_g$ state (thin black curve) in Figure 4(c). According to the dressed potential curves in the left-hand panel, the $2s\sigma_g - 2\omega$ and $2p\sigma_u - 1\omega$ curves overlap around $R = 8.5$ au. When the dissociating population on $2p\sigma_u$ passes the overlapped region, it would be partially excited to $2s\sigma_g$ via absorbing one photon, resulting in the enhancement of the dissociation yield of $2s\sigma_g$. However, our calculation shows that the dissociating population on $2p\sigma_u$ reaches the coupling region at the time of $t \approx 18(2\pi/\omega)$ when the electric field becomes weak at the tail of the pulse; thus, the enhancement for $2s\sigma_g$ is weaker than that in Figure 4(b).

4. Conclusion

In conclusion, the dissociation of $H_2{}^+$ by the UV pulses with various wavelengths has been studied. Our results show that the dissociation into highly excited electronic states becomes significant at some critical photon energies. By calculating the nuclear KER spectra of the dissociation pathways through different electronic states, we have verified the CRE process that leads to the dissociation enhancement. It indicates that the coupling between the lowest two states of $H_2{}^+$ plays an important role in the enhanced disso-

ciation into highly excited states. Though this study focuses on the simplified model of $H_2{}^+$, the essential dynamics of CRE could be generalised to more complicated molecular systems as long as the lowest two states of the molecule are strongly coupled. As the control over electron localisation involving highly excited states has become a subject of interest lately [15,25,30], the CRE process would open a feasible access to achieve efficient control of electron localisation in highly excited states.

References

[1] A.H. Zewail, Science **242**, 1645 (1988).
[2] A. Assion, T. Baumert, M. Bergt, T. Brixner, B. Kiefer, V. Seyfried, M. Strehle, and G. Gerber, Science **282**, 919 (1998).
[3] M.F. Kling, C. Siedschlag, A.J. Verhoef, J.I. Khan, M. Schultze, T. Uphues, Y. Ni, M. Uiberacker, M. Drescher, F. Krausz, and M.J.J. Vrakking, Science **312**, 246 (2006).
[4] P. Lan, E.J. Takahashi, and K. Midorikawa, Phys. Rev. A **83**, 063839 (2011).
[5] F. He, C. Ruiz, and A. Becker, Phys. Rev. Lett. **99**, 083002 (2007).
[6] J.H. Posthumus, Rep. Prog. Phys. **67**, 623 (2004).
[7] F. Martín, J. Fernández, T. Havermeier, L. Foucar, Th. Weber, K. Kreidi, M. Schöfler, L. Schmidt, T. Jahnke, O. Jagutzki, A. Czasch, E.P. Benis, T. Osipov, A.L. Landers, A. Belkacem, M.H. Prior, H. Schmidt-Böking, C.L. Cocke, and R. Döner, Science **315**, 629 (2007).
[8] J.-Ph. Karr, J. Mol. Spectrosc. **300**, 37 (2014).
[9] S. Schiller, D. Bakalov, and V.I. Korobov, Phys. Rev. Lett. **113**, 023004 (2014).
[10] B. Moser and G.N. Gibson, Phys. Rev. A **80**, 041402 (2009).
[11] M. Kremer, B. Fischer, B. Feuerstein, V.L.B. de Jesus, V. Sharma, C. Hofrichter, A. Rudenko, U. Thumm, C.D. Schröter, R. Moshammer, and J. Ullrich, Phys. Rev. Lett. **103**, 213003 (2009).
[12] K. Liu, Q. Zhang, P. Lan, and P. Lu, Opt. Express **21**, 5107 (2013).
[13] P.H. Bucksbaum, A. Zavriyev, H.G. Muller, and D.W. Schumacher, Phys. Rev. Lett. **64**, 1883 (1990).
[14] A. Giusti-Suzor, X. He, O. Atabek, and F.H. Mies, Phys. Rev. Lett. **64**, 515 (1990).
[15] K.P. Singh, Pramana **82**, 87 (2014).
[16] T. Zuo and A.D. Bandrauk, Phys. Rev. A **52**, R2511 (1995).

[17] A. Staudte, D. Pavičić, S. Chelkowski, D. Zeidler, M. Meckel, H. Niikura, M. Schöffler, S. Schössler, B. Ulrich, P.P. Rajeev, T. Weber, T. Jahnke, D.M. Villeneuve, A.D. Bandrauk, C.L. Cocke, P.B. Corkum, and R. Dörner, Phys. Rev. Lett. **98**, 073003 (2007).

[18] C. Huang, P. Lan, Y. Zhou, Q. Zhang, K. Liu, and P. Lu, Phys. Rev. A **90**, 043420 (2014).

[19] G.N. Gibson, L. Fang, and B. Moser, Phys. Rev. A **74**, 041401 (2006).

[20] Z. Wang, K. Liu, P. Lan, and P. Lu, J. Phys. B **48**, 015601 (2015).

[21] J. McKenna, A.M. Sayler, F. Anis, B. Gaire, Nora G. Johnson, E. Parke, J.J. Hua, H. Mashiko, C.M. Nakamura, E. Moon, Z. Chang, K.D. Carnes, B.D. Esry, and I. Ben-Itzhak, Phys. Rev. Lett. **100**, 133001 (2008).

[22] B. Manschwetus, T. Nubbemeyer, K. Gorling, G. Steinmeyer, U. Eichmann, H. Rottke, and W. Sandner, Phys. Rev. Lett. **102**, 113002 (2009).

[23] M. Førre, S. Barmaki, and H. Bachau, Phys. Rev. Lett. **102**, 123001 (2009).

[24] E. Lötstedt, T. Kato, and K. Yamanouchi, J. Chem. Phys. **138**, 104304 (2013).

[25] H. Li, A.S. Alnaser1, X.M. Tong, K.J. Betsch, M. Kübel, T. Pischke, B. Förg, J. Schötz, F. Süßmann, S. Zherebtsov, B. Bergues, A. Kessel, S.A. Trushin, A.M. Azzeer, and M.F. Kling, J. Phys. B **47**, 124020 (2014).

[26] L. Yue and L.B. Madsen, Phys. Rev. A **88**, 063420 (2013).

[27] K. Liu, P. Lan, C. Huang, Q. Zhang, and P. Lu, Phys. Rev. A **89**, 053423 (2014).

[28] X. Zhu, M. Qin, Q. Zhang, Y. Li, Z. Xu, and P. Lu, Opt. Express **21**, 5255 (2013).

[29] Y. Li, W. Hong, Q. Zhang, S. Wang, and P. Lu, Opt. Express **19**, 24376 (2011).

[30] F. He, Phys. Rev. A **86**, 063415 (2012).

[31] K.C. Kulander, F.H. Mies, and K.J. Schafer, Phys. Rev. A **53**, 2562 (1996).

[32] B. Feuerstein and U. Thumm, Phys. Rev. A **67**, 043405 (2003).

[33] C.B. Madsen, F. Anis, L.B. Madsen, and B.D. Esry, Phys. Rev. Lett. **109**, 163003 (2012).

[34] R.E.F. Silva, F. Catoire, P. Rivière, H. Bachau, and F. Martín, Phys. Rev. Lett. **110**, 113001 (2013).

[35] K. Liu, Q. Zhang, and P. Lu, Phys. Rev. A **86**, 033410 (2012).

[36] A. Picón, A. Bahabad, H.C. Kapteyn, M.M. Murnane, and A. Becker, Phys. Rev. A **83**, 013414 (2011).

[37] N. Takemoto and A. Becker, Phys. Rev. Lett. **105**, 203004 (2010).

[38] K.J. Schafer and K.C. Kulander, Phys. Rev. A **42**, 5794 (1990).

[39] F. Catoire and H. Bachau, Phys. Rev. A **85**, 023422 (2012).